Optical Materials 47 (2015) 72–77

Contents lists available at ScienceDirect

Optical Materials

journal homepage: www.elsevier.com/locate/optmat

Holographic gratings recorded in poly(lactic acid)/azo-dye films

Javier Cambiasso [a], Silvia Goyanes [b], Silvia Ledesma [a,*]

[a] Image Processing Laboratory (LPI), Physics Department, FCEyN, UBA, Ciudad Universitaria 1428, Ciudad Autónoma de Buenos Aires, Argentina
[b] Laboratory of Polymers and Composite Materials (LP&MC), Physics Department and IFIBA-CONICET FCEyN-UBA, Ciudad Universitaria 1428, Ciudad Autónoma de Buenos Aires, Argentina

ARTICLE INFO

Article history:
Received 10 April 2015
Received in revised form 12 May 2015
Accepted 1 June 2015
Available online 7 July 2015

Keywords:
Azobenzene
Diffraction gratings
Efficiency enhancement

ABSTRACT

Diffraction gratings were recorded in biodegradable polymer films of poly(lactic acid) doped with the photoisomerisable azo-dye (Disperse Orange 3). It is shown that the diffraction efficiency of the recorded grating can be improved by 220% via an all-optical treatment. This all-optical treatment consists of a pre-irradiation of the sample with the writing laser beam at high power during a short period of time, preventing damage of the material, followed by a much longer inscription at relatively low power. Furthermore, it is shown that the addition of a small amount of 0.05 wt% of multi-walled carbon nanotubes to the photoresponsive polymer increases the maximum diffraction efficiency as well as the remanent efficiency by 20%. Finally, this last photoresponsive nano-composite is also sensitive to the pre-irradiation treatment.

1. Introduction

Holographic data recording devices promise to be the next generation of high-density ultra-fast storage memories [1]. Optical memories are being investigated because they offer the possibility of storing higher density of data in comparison with the more conventional media such as CDs, DVDs or Blue-ray disks. Furthermore, the retrieval of information could also be accelerated because holographic media can store whole pages of information in the entire volume of the material, allowing for many pages of data to be registered and read at once [2].

Many materials are known where holographic data can be stored. In particular, azobenzene containing polymers have been shown to be appropriate candidates for storage media [3–6]. These photosensitive polymers respond both to the spatial variation of intensity and to the polarisation of the recording light, giving rise to more degrees of freedom than conventional intensity sensitive materials for applications in holographic storage. Diffraction gratings are the building blocks of the holographic technology, thus proving the possibility of recording them in these material is a huge step into the potential application of optical memories.

Now, these intensity and polarisation dependent properties arise as a consequence of the azobenzene photochemistry [7–9]. Upon absorption of a linearly polarised photon, with the required energy to induce electronic transitions in the molecule, the azobenzene isomerises from the thermodynamically stable *trans* state into the *cis* form changing its morphology and its dipole moment [10]. The back transformation can also be caused by absorption of another photon with the appropriate energy or by thermal relaxation in a timescale several orders of magnitude higher than its optical counterpart [11]. After repeated *trans–cis–trans* photoisomerisation cycles the molecules will end up oriented perpendicularly to the polarisation axis of the actinic light. The molecular reorientation that occurs due to the polarisation of light is also dependent on the intensity of the excitation beam. As a consequence of this nanoscopic alignment, the macroscopic electric susceptibility of the bulk material changes and with it, birefringence [12,13] and dichroism [14] can be induced in the material. Other effect that could be observed in these materials is the modulation of the surface due to a microscopic mass-transport of the polymeric chains driven by the same photoinduced orientation of the chromophores [15–18]. This phenomenon is detrimental to holographic applications where volume recording is sought, but it can be exploited in nanopatterning and photolithographic applications [19].

The maximum birefringence induced by photoisomerisation phenomena depends both on the intensity and polarisation of the writing beam. However many materials present relatively low birefringence, despite optimisation of the optical parameter. Thus, considerable effort has been centred in developing materials or techniques which could improve the induced photoanisotropy. For example, the optical anisotropy was increased with varying

* Corresponding author.
E-mail addresses: goyanes@df.uba.ar (S. Goyanes), ledesma@df.uba.ar (S. Ledesma).

http://dx.doi.org/10.1016/j.optmat.2015.06.002
0925-3467/

the working temperature, as shown in Refs. [20,21]. It was also shown that the addition of a small amount of multi-walled carbon nanotubes to a photosensitive poly(lactic acid) doped homopolymer [21] could also be used to increase the induced birefringence. Furthermore, it has been shown [22] that irradiating a non biodegradable poly(methyl methacrlate)/Disperse Red 1 covalently functionalised azopolymer with an assisting polarised UV or visible beam while generating the diffraction grating, can further accelerate the photoisomerisation process and, simultaneously, the diffraction grating recording. This protocol is easily applicable for it involves an all-optical non-invasive algorithm to achieve a faster recording of the diffraction grating.

With regards to the polymeric matrix, most studies have been carried out on PMMA polymers, whose glass transition temperatures (T_g) is relatively higher than room temperature. In addition, PMMA is not biodegradable, which renders it highly unsuitable for the current environmentally concerned regulations. In order to meet these demands, other works have been made on poly(vinyl alcohol) (PVA) which is a biodegradable polymer with a relatively high T_g. Another alternative could be poly(lactic acid) (PLA), which has an elastic modulus and a stress at break higher than PVA and is optically transparent, which makes it enticing for optical applications.

Our group has already studied the optical properties of two PLA photoresponsive films: PLA containing Disperse Orange 3 (DO3) as azo-dye and a composite of PLA-DO3 containing 0.06 wt% of multi-walled carbon nanotubes (MWCNTs) [21]. It was shown that optical anisotropy could be induced in these materials and that the birefringence was improved by the addition of a small amount of MWCNTs. Because the simplicity of the preparation method these guest–host photoresponsive systems can be produced in industrial scale.

To our knowledge the ability to record diffraction holographic gratings in PLA/dye has not been demonstrated yet. In this work, the optical anisotropy was exploited to record diffraction gratings in thin PLA/DO3 films. Also, the existence of surface modulation was studied and the possibility of enhancing its efficiency by means of a simple optical treatment was explored. It should be emphasised that in this treatment the material is exposed mainly to low intensity light during most of the inscription, thus preventing irreversible damage, which could be caused by a long exposure to high intensity lasers on the material. Inspired on the previous reported result, samples of PLA/DO3 with a small amount of MWCNTs were also analysed. The obtained results indicate that these materials, which are approximately 90% biodegradable, could be used as optical storage devices based on highly renewable sources.

2. Experimental

Two different mostly biodegradable materials were prepared. One of them was a mixture of PLA as the host polymer containing 9.10 wt% of DO3 as the photoisomerizable azo-dye. The other one was PLA with 9.05 wt% of DO3 and 0.05 wt% of MWCNTs. The former material will be referred to as PLA/DO3 and the latter as PLA/DO3/MWCNTs.

2.1. Materials

Pellets of PLA (10% D-Lactide, 90% L-Lactide), manufactured by Shenzhen Bright China Industrial Co. Ltd (Wuhan, China), were used as the matrix polymer. The weight and number averaged molecular weight of the polymer are 67,600 g mol^{-1} and 49,900 g mol^{-1}, respectively. DO3 dye was purchased from Sigma–Aldrich and used as received. Fig. 1 shows the chemical structure of both the azo-dye and the polymer matrix. MWCNTs were obtained from Nanocyl (NC3100). Their length is about 1.5 μm and their diameter is around 20–40 nm.

The MWCNTs were kept in a vacuum oven until use. The solvent used was Chloroform because both DO3 and PLA are soluble in it and, furthermore, it was already noticed that MWCNTs can be dispersed in a DO3/chloroform solution [23]. Reagent grade chloroform was purchased from Biopack (Argentina) and used as received.

2.2. Film preparation

2.2.1. Photoresponsive PLA (PLA/DO3)

Photoresponsive PLA was prepared according to the following protocol. 0.05 g of DO3 were dissolved in 12.5 mL of Chloroform and sonicated for 10 min. Then, 0.5 g of PLA where added to the solution. This results in a final concentration of 9.1 wt% for the PLA/DO3 mixture. This solution was later sonicated for another 20 min. Several samples were made by spin-coating 100 μL of solution into a previously cleaned coverslip at a rotating speed of 2200 rpm. The films were dried in a vacuum oven for 12 h at 60 °C. Thin films of (0.9 ± 0.1) μm were obtained.

2.2.2. Photoresponsive nano-composite (PLA/DO3/MWCNTs)

A similar protocol was used to produce thin films of photoresponsive nano-composites. A small amount of MWCNTs (0.3 mg) was mixed with 0.05 g of DO3 and dissolved in Chloroform. After 10 min of sonication 0.5 g of PLA and 0.05 g of DO3 were added to the mixture. This ensures that the sample has a final concentration of approximately 9.05 wt% of DO3 and 0.05 wt% of MWCNTs. Finally, the solution was sonicated for another 20 min. Thin films were fabricated by spin-coating 100 μL of the solution into a previously cleaned coverslip at a rotating speed of 2200 rpm. The films were dried in a vacuum oven for 12 h at 60 °C. Thin films of (0.9 ± 0.1) μm were obtained.

2.3. Diffraction grating recording

A diffraction grating can be recorded in thin photoresponsive films using a Lloyd interferometer, as previously reported [13,24,25,18]. The experimental setup used is shown in Fig. 2. The writing beam (a solid state LRS-473-TM-50-5 laser operating at 473 nm, coherence length around 1.5 mm) was spatially filtered and collimated using the microscope objective O, pinhole PH and

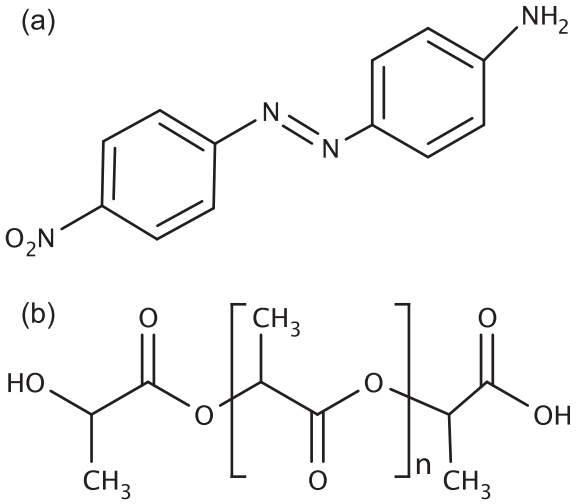

Fig. 1. Chemical structure of (a) the azo-dye DO3, (b) the polymer matrix PLA.

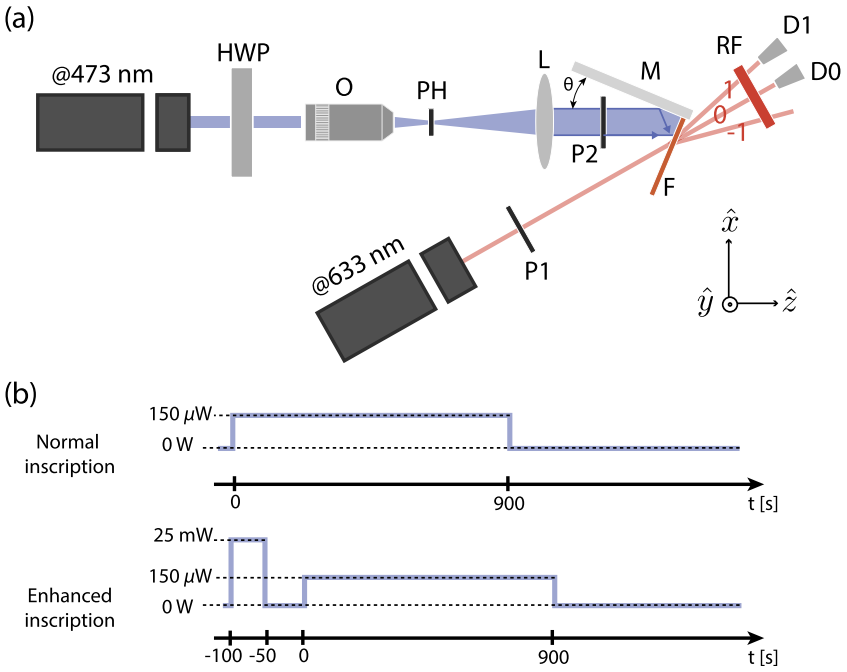

Fig. 2. (a) Experimental setup used to record a diffraction grating on the film and measure the diffraction efficiency. (b) Two different excitation protocols used to record the gratings. The lines represent the power of the writing beam. (Axes not to scale).

lens L. The half-wave plate (HWP) and the polarizer P2 were used to control the inscription power on the sample. The intensity of the writing beam arriving at the sample was measured using a Newport 1918-R calibrated photodetector. At this stage half the wavefront impinges on the sample and the other half is reflected at an angle θ from a mirror M. An interference pattern appears on the plane perpendicular to the mirror as a consequence of the superposition of both coherent wavefronts. The period Λ of this pattern is given by Bragg's condition:

$$\Lambda = \frac{\lambda_w/2}{\sin\theta}, \tag{1}$$

where $\lambda_w = 473$ nm is the writing beam wavelength. In this work a period of about 3 μm was used, which corresponds to a Bragg angle of 4.5. We have selected a low enough period grating to show the feasibility of the method in applications in holographic media.

The superposition of two electromagnetic waves gives rise to an intensity modulated pattern (IMP). In some situations where the polarization states of both beams differ or are orthogonal a polarization modulated pattern (PMP) is obtained [13,19]. The influence of each modulation pattern on the azopolymer can be studied independently by choosing a suitable polarization state for the writing beam. In this work, the polarization state of the writing beam was chosen to be at 45° of the y-axis (see Fig. 2a). The resulting interference pattern consisted of a pure polarization modulation. The intensity of the writing beam impinging on the sample was varied as explained below.

The reading beam, a He–Ne laser, was used to probe the dynamics of the recording process. After passing through polarizer P1 it impinged on the sample. Once a diffraction grating is successfully recorded on the material, the reading beam diffracts, given rise to several diffracted orders. The intensity of the +1 (or −1) diffracted order (measured at detector D1) relative to the 0th order (measured at detector D0) provides a global parameter to quantify the grating inscription process and is called the diffraction efficiency η.

The used inscription protocol can be divided into three different stages as shown in Fig. 2b. First of all, a writing beam of 270 mW cm^{-2} was used to excite the sample during 50 s. Then, the material was left to relax during another 50 s. Finally, the intensity of the writing beam was diminished to 1.6 mW cm^{-2}.

This low intensity actinic light was used to record the grating for 900 s, which resulted to be enough time to fit the data with low uncertainty in the parameters related to the slower dynamic processes. In the following, the first two of these stages (−100 s to 0 s in Fig. 2b enhanced inscription protocol) will be referred to as the all-optical treatment stage, whereas the last one will be called the enhancement stage. One advantage of using this protocol is that the sample is mostly illuminated with low intensity light, which prevents damage to the material caused by a prolonged exposure to high intensity light.

In order to compare the enhanced evolution of the diffraction efficiency with the ordinary diffraction efficiency dynamics, a low inscription intensity of 1.6 mW cm^{-2} was used to record another diffraction grating.

3. Results

3.1. Photoresponsive PLA and all-optical enhancement

Fig. 3 shows the first order diffraction efficiency of the recorded grating in the photoresponsive PLA material. It demonstrates that it is possible to record a grating in the material, however, atomic force microscopy revealed no surface modulation, indicating that the register is made in volume. When the actinic light was turned off the material relaxes producing a decrease in the diffraction efficiency.

In the same figure the recorded grating after the all-optical treatment stage is shown. It can be seen that, compared to the case with no treatment, a faster response and a higher value of both the saturation and remanent diffraction efficiency are obtained.

In order to quantify this phenomenon the diffraction efficiencies curves are usually fitted with complex Bessel functions [26], but for the purpose of this article we will assume a much easier phenomenological model as used in Refs. [27,28] that take into account slow and fast molecular dynamics. These curves are simple biexponential functions of the form:

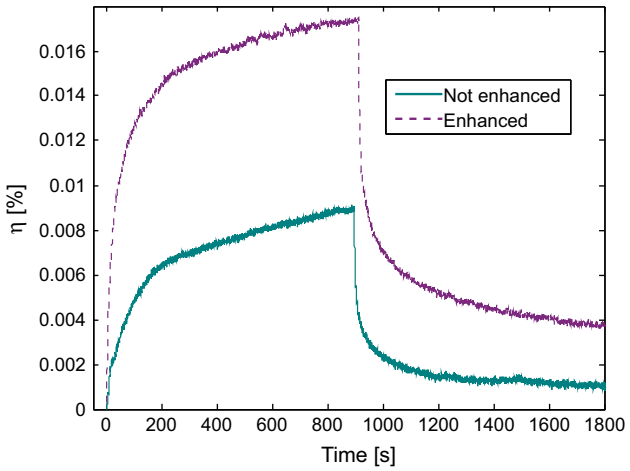

Fig. 3. Comparison between enhanced and ordinary diffraction efficiencies in a PLA/DO3 film.

$$\Delta\eta_{\uparrow}(t) = A\left(1 - e^{-t/\tau_a}\right) + B\left(1 - e^{-t/\tau_b}\right), \tag{2a}$$

$$\Delta\eta_{\downarrow}(t) = Ce^{-t/\tau_c} + De^{-t/\tau_d} + E, \tag{2b}$$

where $\Delta\eta_{\uparrow}(t)$ and $\Delta\eta_{\downarrow}(t)$ are the first order diffraction efficiencies during the writing and relaxation intervals, $A - E$ constants indicating the intensity of the diffraction efficiencies and $\tau_a - \tau_d$ characteristic times of the inscription. Table 1 summarizes the results obtained by fitting these equations to the data.

The main differences are summarized as follows:

1. The saturation level of the enhanced diffraction efficiency is 55% higher than that of the not-enhanced.
2. The enhanced diffraction efficiency has fast (τ_a) time 25% smaller, indicating faster recording dynamics.
3. The remanent diffraction efficiency at the enhanced stage is 220% higher than the not-enhanced remanent value.

Given that both the enhanced and not-enhanced measurements were performed under the same conditions (same laser power for both writing and reading processes and same sample), it could be assumed that the increment in the diffraction efficiency is only related to the number of active azo dyes. The optical treatment produces an activation of the previously inactive molecules leading to an increment of the population of photoisomerizable azo-dyes.

It is well known that the azo dye present in the sample is inhibited to isomerize if certain restrictions on the free volume are not met. The molecule requires enough free space to induce the cycle between the *trans* and *cis* states [29,30]. Other mechanism that could hinder this photoisomerization are, for example, the interaction between the amino terminal group of the DO3 molecule and the ester group of the PLA [31,32]. This interaction corresponds to a more compact arrangement of the azo-dye, reducing the free volume for photoisomerization and confining DO3 molecules to the neighbourhood of the polymeric matrix. As a consequence, these chromophores lack the needed free-volume to photoisomerize. However, the high-intensity writing laser at the all-optical treatment stage seems to have delocalized and thus optically activated the initially confined chromophores by breaking their interaction to the polymeric matrix. The higher saturation value of the enhanced diffraction efficiency can be attributed to this net increase of the effective chromophore population.

Besides, the remanent diffraction efficiency is also enhanced after the all-optical treatment stage. This result can be explained as follows. A higher diffraction efficiency, as stated before, could be related to a higher amount of ordered chromophores. The van der Waals interactions between molecules aid at stabilising the ordered lattice. A similar effect can be observed in ferromagnetic substances. As is well-known, when an ordered n-dimensional ($n \geqslant 2$) lattice of aligned spins is created, the whole system remains stable under small perturbations [33].

The remanent enhanced diffraction efficiency achieves a 220% higher asymptotic value compared to the not-enhanced one. As was previously explained, this suggests that a higher level of aligned molecules was obtained, making the whole ordered structure more stable, thanks to the van der Waals interactions between the aligned molecules.

Regarding the velocity of the process, Table 1 shows that the characteristic time (τ_a), associated to the azo-dye, is around 25% smaller in the enhanced sample, indicating an increase in azo-dye mobility.

This would indicate that the high-intensity exciting light increases the temperature of the sample, which was later confirmed by measuring the bulk temperature of the film with a thermocouple. The temperature was observed to increase around 15 °C during the inscription but room temperature was achieved again after the first 40–50 s of the relaxation period. Therefore, the temperature of the film (and thus, the mean free volume distribution in the film) is comparable in both enhanced and not-enhanced inscriptions.

During the enhancement process (−100 s to −50 s in Fig. 2b) the temperature increases up to 15 °C over room temperature (20 °C). When the laser is turned off (at −50 s in Fig. 2b) the sample temperature decreases to room temperature in about 30 s, which guarantees that the sample is at room temperature when the second stage of the process begins (at 0 s in Fig. 2b). Taking into account that the T_g of this material is 50 °C [32] the maximum temperature achieved after the pre-irradiation is lower than the material glass transition temperature but is enough to guarantee that during this short period of time in which the material is heated the free volume suffers a small increase. As a consequence the azo-dye molecules experiment an enhanced mobility.

Then, the main difference between the enhanced and not-enhanced inscriptions is that they begin with other initial populations of *cis* and *trans* chromophores. After the enhancement stage, the high-intensity writing excitation at 473 nm produces an increase in the population of *cis* isomers as stated by Liu et al. [34]. This excitation wavelength is associated with the $\pi \rightarrow \pi^*$ transition band, which is stronger for the *trans* isomer. Thus, at the enhanced stage, the film contains a higher amount of *cis* molecules, which have not yet thermally relaxed. In order to demonstrate the high concentration of *cis* isomers in the treated

Table 1
Adjustment parameters of Figs. 3 and 5 using Eq. (2). Diffraction efficiencies η_{sat} and η_{rem} are shown in [%] and the characteristic times $\tau_a - \tau_d$ in [s].

	η_{sat}	τ_a	τ_b	η_{rem}	τ_c	τ_d
PLA/DO3	1.1 ± 0.1	33 ± 4	370 ± 40	0.11 ± 0.02	9 ± 3	150 ± 20
PLA/DO3 Enh.	1.7 ± 0.2	25 ± 4	250 ± 30	0.35 ± 0.01	14 ± 3	270 ± 30
PLA/DO3/MWCNTs	1.3 ± 0.1	42 ± 5	280 ± 30	0.21 ± 0.01	12 ± 2	300 ± 30
PLA/DO3/MWCNTs Enh.	2.1 ± 0.2	21 ± 4	270 ± 40	0.43 ± 0.01	13 ± 2	270 ± 30

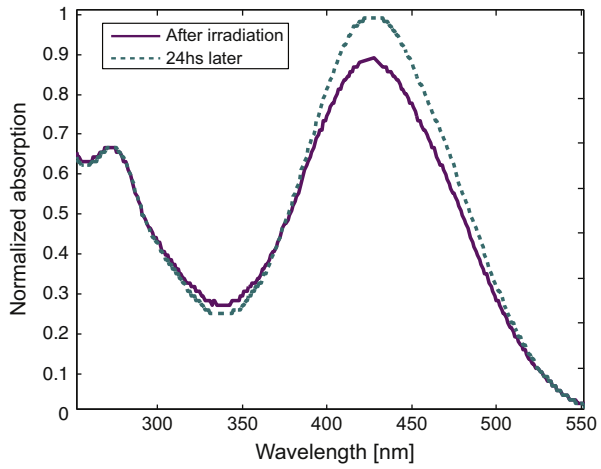

Fig. 4. Spectra obtained just after irradiation of 250 mW cm^{-2} at 473 nm and after 24 h of thermal relaxation.

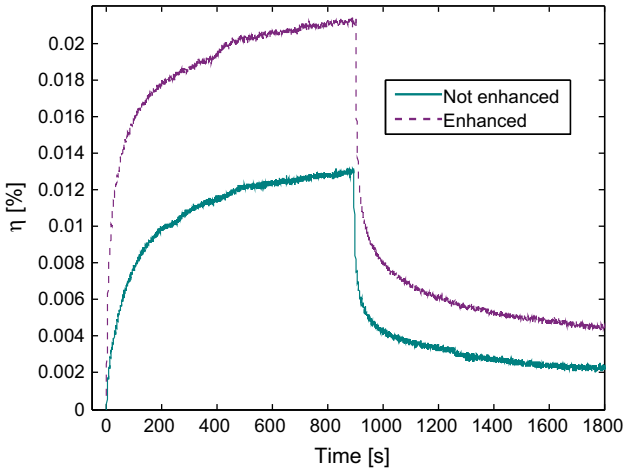

Fig. 5. Comparison between enhanced and ordinary diffraction efficiencies in a PLA/DO3/MWCNTs film.

samples an UV–vis study was performed. Fig. 4 shows the differences in the UV–vis spectrum of the same PLA/DO3 film just after treatment and 24 hs after it. The initially *cis*-rich sample, after enough time to thermally relax, increased the population of the *trans* isomer, thus rendering the $\pi \rightarrow \pi^*$ band around 420 nm stronger. This phenomenon was previously observed in other experiments studying different samples [35,36,34], where it was stated that this band is related to the $\pi \rightarrow \pi^*$ transitions of the trans and *cis* isomers.The increase of the *cis* isomer in the sample accelerates the inscription process due to its higher quantum yield at the inscription wavelength [7,37]. In other words, a molecule in the *cis* configuration is more easily photoisomerizable, because it is already in a metastable state. Thus, an initial faster response to the nanoscopic alignment of molecules can be observed.

It is interesting to note that the reported effect is more important when MWCNTs are added to the sample, as shown in the following section.

3.2. Photoresponsive nano-composite and all-optical enhancement

It was already reported that the optically induced birefrigence in PLA/DO3 materials could be enhanced by adding a small amount of MWCNTs [21]. This motivated the idea that a higher diffraction efficiency could also be obtained. Accordingly, holographic gratings were recorded in the PLA/DO3/MWCNTs films and the first order diffraction efficiency is shown in Fig. 5. Similarly, no surface corrugation was observed in this materials. This curve was fitted by Eq. (2) and the parameters of this fit are shown in Table 1. Compared with PLA/DO3 sample Moreover the saturation and the remanent diffraction efficiencies were amplified by around 20% in both cases, only by adding 0.05 wt% of MWCNTs.

As was previously shown [21] the addition of MWCNTs to the photosensitive polymer diminished the glass transition temperature (T_g) of the material. Both the MWCNTs and the DO3 dye interact via π–π stacking [23]. This interaction would keep DO3 molecules in the neighbourhood of the MWCNTs, preventing them from being confined within the PLA chains. As a consequence, the packing density of the azobenzene molecules changes. Moreover, the addition of MWCNTs changes the overall arrangement of PLA chains due to steric hindrance. This generates a larger free volume size distribution, enabling DO3 molecules to increase their mobility [32].

The enhancement effect produced by the all optical is also observed in these materials as can be seen in Fig. 5 and the parameters reported in Table 1, showing a doubling in both the saturation and remanent diffraction efficiencies and a decrease in half of the fast inscription time.

4. Conclusions

Holographic gratings were recorded in mostly biodegradable PLA polymers containing DO3. The diffraction efficiency was low but measurable corresponding to a successful recording of a periodic structure on the volume of the material without surface modulation. An improvement of the diffraction efficiency was obtained via a simple all-optical treatment.This enhancement consists of higher saturation and remanent values of the diffraction efficiency, in addition to a decrease in the recording times necessary to achieve the saturation diffraction efficiency. These results were explained by considering the availability of DO3 molecules initially confined to the polymer matrix, but activated after the all-optical treatment stage. Finally the diffraction efficiency can be further increased by adding a small amount of MWCNTs to the sample. It was also shown that, in this materials, the all optical treatment improves the diffraction efficiency just like in the case of the PLA/DO3 film. It should be noted that, thanks to the proposed enhancement protocol, which diminishes the inscription times, it is not necessary to expose the sample to prolonged irradiation times with high intensity lasers, thus preventing damages in the material.

Acknowledgements

The authors want to thank the National Scientific and Technical Research Council of Argentina, CONICET (11220080103047, PIP 2013-2015 and 11220120100508CO), the University of Buenos Aires (UBACYT 2011-2014, 20020100100689 and 200201001 00350) and ANPCyT (PICT 2010-02179 and PICT-2012-1093), for their support.

References

[1] F.K. Bruder, H. Rainer, T. Rölle, M.S. Weiser, T. Fäcke, From the surface to volume: concepts for the next generation of optical-holographic data-storage materials, Angew. Chem. Int. Ed. 50 (2011) 4552–4573.
[2] G.T. Sincerbox, History and physical principles, in: H.J. Coufal, D. Psaltis, G.T. Sincerbox (Eds.), Holographic data storage, Springer Series in Optical Sciences, Springer-Verlag, 2000, pp. 3–20.
[3] Y. Zhao, T. Ikeda, Smart Light-responsive Materials, Wiley, 2009.

[4] X. Pan, C. Wang, C. Wang, X. Zhang, Image storage based on circular-polarization holography in an azobenzene side-chain liquid-crystlaline polymer, Appl. Opt. 47 (1) (2008) 93–98.
[5] H. Ono, K. Suzuki, T. Sasaki, T. Iwato, A. Emoto, T. Shioda, N. Kawatsuki, Reconstruction of polarized optical images in two- and three-dimensional vector holograms, J. App. Phys. 106 (2009).
[6] T. Sasaki, M. Izawa, K. Noda, E. Nishioka, N. Kawatsuki, H. Ono, Temporal formation of optical anisotropy and surface relief during polarization holographic recording in polymethylmethacrylate with azobenzene side groups, Appl. Phys. B 114 (3) (2014) 373–380.
[7] H. Rau, Photoisomerization of azobenzenes, in: J.F. Rabek (Ed.), Photochemistry and Photophysics, CRC Press, 1990, pp. 3–47. Ch. 1.
[8] O.N.J. Oliveira, D.S. dos Santos Jr., D.T. Balgoh, V. Zucolotto, C. Mendonça, Optical storage and surface-relief gratings in azobencene-containing nanostructured films, Adv. Colloid Interface Sci. 116 (2005) 179–192.
[9] H.M. Dhammika Bandara, S.C. Burdette, Photoisomerization in different classes of azobenzene, Chem. Soc. Rev. 41 (2012) 1809–1825.
[10] N.S. Allen (Ed.), Handbook of Photochemistry and Photophysics of Polymer Materials, Wiley, 2010.
[11] Z. Mahimwalla, K.G. Yager, J. Mamiya, A. Shishido, A. Priimagi, C.J. Barrett, Azobenzene photomechanics: prospects and potential applications, Polym. Bull. 69 (2012) 967–1006.
[12] T. Todorov, L. Nikolova, N. Tomova, Polarization holography. 1: a new high-efficiency organic material with reversible photoinduced birefringence, App. Opt. 23 (1984).
[13] P.S. Ramanujam, L. Nikolova, Polarization Holography, 1st ed., Cambridge Univ. Press, 2009.
[14] P. Rochon, J. Gosselin, A. Natansohn, S. Xie, Optically induced and erased birefringence and dichroism in azoaromatic polymers, Appl. Phys. Lett. 60 (1) (1992) 4–5.
[15] D.Y. Kim, S.K. Tripathy, L. Li, J. Kumar, Laser-induced holographic surface relief gratings on nonlinear optical polymer films, Appl. Phys. Lett. 66 (10) (1995) 1166–1168.
[16] N.K. Viswanathan, D.Y. Kim, S. Bian, J. Williams, W. Liu, L. Li, L. Samuelson, J. Kumar, S.K. Tripathy, Surface relief structures on azo polymer films, J. Mater. Chem. 9 (1999) 1941–1955.
[17] B.M. Schultz, M.R. Huber, T. Bieringer, G. Krausch, S.J. Zilker, Lenfth-scale dependence of surface relief gratings in azobenzene side-chain polymers, Synthetic Metals 124 (2001) 155–157.
[18] J.E. Koskela, J. Vapaavuori, J. Hautala, A. Priimagi, C.F.J. Faul, M. Kaivola, R.H.A. Ras, Surface-relief gratings and stable birefringence inscribed using light of broad spectral range in supramolecular polymer-bisazobenzene complexes, J. Phys. Chem. C 116 (2012) 2363–2370.
[19] A. Kravchenko, A. Shevchenko, P. Grahn, V. Ovchinnikov, M. Kaivola, Photolithographic periodic patterning of gold using azobenzene-functionalized polymers, Thin Solid Films (2013).
[20] F. Dall' Agnol, J.R. Silva, S.C. Zílio, O.N.J. Oliveira, J.A. Giacometti, Temperature dependence of photoinduced birefringence in polystyrene doped with disperse red-1, Macromol. Rapid. Commun. 23 (2002) 948–951.
[21] G. Díaz Costanzo, L. Ribba, S. Goyanes, S. Ledesma, Enhancement of the optical response in a biodegradable polymer/azo-dye film by the addition of carbon nanotubes, J. Phys. D: Appl. Phys. 47 (13) (2014) 135103.
[22] X. Wu, T.T. Ngan Nguyen, I. Ledoux-Rak, C.T. Nguyen, N.D. Lai, Optically accelerated formation of one- and two-dimensional holographic surface relief gratings on dr1/pmma, in: Holography – Basic Principles and Contemporary Applications, 2013.
[23] G. Díaz Costanzo, S. Ledesma, I. Mondragon, S. Goyanes, Stable solutions of multiwalled carbon nanotubes using an azobenzene dye, J. Phys. Chem. C 114 (2010) 14347–14352.
[24] F. Lagugné-Labarthet, T. Buffeteau, C. Sourisseau, Azopolymer holographic diffraction gratings: time dependent analyses of the diffraction efficiency, birefringence, and surface modulation induced by two linearly polarized interfering beams, J. Phys. Chem. B 103 (1999) 6690–6699.
[25] P. Rochon, E. Batalla, A. Natansohn, Optically induced surface gratings on azoaromatic polymer films, Appl. Phys. Lett. 66 (2) (1995) 136–138.
[26] A. Sobolewska, S. Bratkiewicz, A. Miniewicz, E. Schab-Balcerzak, Polarization dependence of holographic grating recording in azobenzene-functionalized polymers monitored by visible and infrared light, J. Phys. Chem. B 114 (2010) 9751–9760.
[27] A. Natansohn, P. Rochon, Photoinduced motions in azo-containing polymers, Chem. Rev. 102 (2002) 4139–4175.
[28] F. Lagugné-Labarthet, F. Labarthet, T. Buffeteau, C. Sourisseau, Optical erasures and unusual surface reliefs of holographic gratings inscribed on thin films of an azobenzene functionalized polymer, Phys. Chem. 4 (2002) 2020–2029.
[29] E. Heydari, E. Mohajerani, A. Shams, All optical switching in azo-polymer planar waveguide, Opt. Commun. 284 (2011) 1208–1212.
[30] T. Bieringer, Photoaddressable polymers, in: H.J. Coufal, D. Psaltis, G.T. Sincerbox (Eds.), Holographic data storage, Springer Series in Optical Sciences, Springer-Verlag, 2000, pp. 209–230.
[31] K. Tawa, K. Kamada, T. Sakaguchi, K. Ohta, Local environment dependence of photoinduced anisotropy observed in azo-dye-doped polymer films, Polymer 41 (9) (2000) 3235–3242.
[32] A.R. Luca, I.A. Moleavin, N. Hurduc, M. Hamel, L. Rocha, Mass transport in low t_g azo-polymers: effect on the surface relief grating induction and stability of additional side chain groups able to generate physical interactions, Appl. Surface Sci. 290 (2014) 172–179.
[33] K. Huang, Statistical Mechanics, 2nd ed., Wiley, 1987.
[34] Y.J. Liu, H.T. Dai, X.W. Sun, Holographic fabrication of azo-dye-functionalized photonic structures, J. Mat. Chem. 21 (2011) 2982–2986.
[35] A. Yavrian, K. Asatryan, T. Galstian, M. Piché, Real-time holographic image restoration in azo dye doped polymer films, Opt. Commun. 251 (2004) 286–291.
[36] D. Aronzon, E.P. Levy, P.J. Collings, A. Chanishvill, G. Chilaya, G. Petriashvily, Trans-cis isomerization of an azoxybenzene liquid crystal, Liquid Crystals 34 (6) (2007) 707–718.
[37] P. Bortolus, S. Monti, Cis–trans photoisomerization of azobenzene. Solvent and triplet donor effects, J. Phys. Chem. 83 (6) (1979) 648–652.